CHALMERS
UNIVERSITY OF TECHNOLOGY

Impact of Intercore Crosstalk on the Transmission Distance of QAM Formats in Multicore Fibers

IEEE Photonics Journal
An IEEE Photonics Society Publication

Open Access

Impact of Intercore Crosstalk on the Transmission Distance of QAM Formats in Multicore Fibers

Volume 8, Number 2, April 2016

B. J. Puttnam
R. S. Luís
T. A. Eriksson
W. Klaus
J.-M. Delgado Mendinueta
Y. Awaji
N. Wada

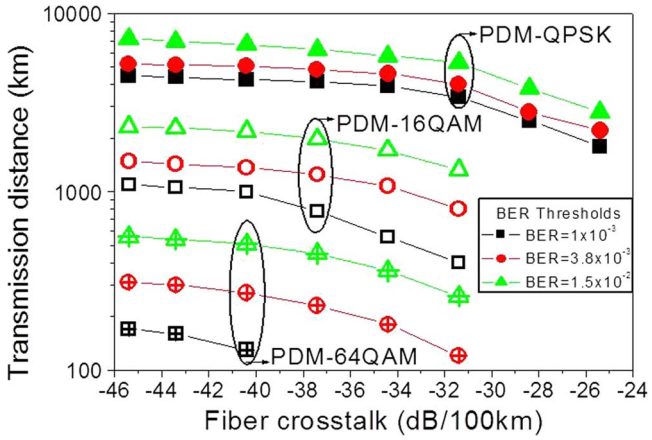

DOI: 10.1109/JPHOT.2016.2523993
1943-0655 © 2016 IEEE

IEEE photonics SOCIETY

IEEE

Impact of Intercore Crosstalk on the Transmission Distance of QAM Formats in Multicore Fibers

B. J. Puttnam,[1] R. S. Luís,[1] T. A. Eriksson,[2] W. Klaus,[1] J.-M. Delgado Mendinueta,[1] Y. Awaji,[1] and N. Wada[1]

[1.] Photonic Network Systems Laboratory, National Institute of Information and Communications Technology (NICT), Tokyo 184-8795, Japan
[2.] Department of Microtechnology and Nanoscience, Chalmers University of Technology, 412 96 Gothenburg, Sweden

DOI: 10.1109/JPHOT.2016.2523993

Manuscript received December 4, 2015; revised January 19, 2016; accepted January 19, 2016. Date of publication February 11, 2016; date of current version April 15, 2016. Corresponding author: B. J. Puttnam (e-mail: ben@nict.go.jp).

Abstract: We investigate the impact of intercore crosstalk on the achievable transmission distance of three square quadrature amplitude modulation (QAM) formats. We show that increasing intercore crosstalk across an 18 dB range starting from –43.4 dB/100 km reduces the achievable transmission distance for all formats, with a greater impact on higher order modulation formats. For a crosstalk level arising from equal signal launch power in each core of a homogeneous 7-core fiber, we measure a reduced transmission distance at BER $= 1.5 \times 10^{-2}$ of 24%, 38% and 54%, for polarization-division-multiplexed-quadrature phase-shift keying (PDM-QPSK), PDM-16QAM, and PDM-64QAM, respectively. Finally, we investigate the potential impact that dynamic crosstalk variation could have in transmission systems based on multicore fiber and estimate the achievable reach for an outage probability of 1×10^{-5} in the presence of dynamically varying intercore crosstalk.

Index Terms: Multi-core fibers, transmission, crosstalk.

1. Introduction

Space-division multiplexing (SDM) technology has been widely investigated as a means of increasing capacity both for long haul transmission [1], [2] and short-range links in access networks and data-centers [1], [3]. In particular, multi-core fiber (MCF) technology is rapidly maturing with a number of high capacity transmission demonstrations [4]–[8], a range of spatial fiber coupling [9]–[11] and amplifier [12]–[14] technologies, and investigations of MCF systems [15], [16] designed to further increase resource sharing and performance.

As is also the case with modes in multi-mode transmission [17], [18], one potential limitation of SDM systems is crosstalk (XT) between spatial channels with various strategies employed to minimize the impact of core-to-core interaction in MCF transmission [19], [20]. This inter-core XT (IC-XT) arises from power coupling between cores during propagation, according to the mode overlap integral [21], [22] and in contrast to in-band XT from other optical components, splices, connectors and amplifiers, is distributed along the fiber link. Furthermore, IC-XT has been shown to have a time varying random frequency dependence [23], [24]. As such, complex

interference mechanisms may affect transmission differently than in-band XT added at a single point, as was investigated by simulation in [25].

Previously, the impact of crosstalk during transmission was investigated for 10 GBd polarization-division-multiplexed (PDM) quadrature phase shift-keying (QPSK) and it was found that a IC-XT level equivalent to launching equal power in all cores of a 7-core MCF limits the transmission distance by up to 25% [26]. Here, we expand on experimental results in [27] and investigate the impact of IC-XT in MCF transmission for square PDM quadrature-amplitude-modulation (QAM) formats up to 64QAM at 25 GBd. We show that the impact of IC-XT becomes more severe for higher order modulation formats with the transmission distance of 64QAM being reduced by as much as 56% at BER $= 3.8 \times 10^{-3}$ at the XT level of 32.2 dB/100 km obtained when launching equal signal launch power in to each core of the homogeneous 7-core MCF used.

Finally, we analyze the potential impact that the dynamic nature of IC-XT may have on the long-term performance of MCF transmission systems. Using assumptions derived from experimental measurements together with a statistical model of crosstalk fluctuations, we estimate an outage probability [28] for MCF fiber systems. For each of the QAM formats investigated, we calculate an additional worst case limitation of transmission distance for specific outage probability of 1×10^{-5}, showing that, particularly for high order modulation, guaranteeing low outage probabilities in the presence dynamic crosstalk behavior can lead to significant reduction in achievable transmission distances.

These results show that for the range values investigated (–43.4 dB/ 100 km to 25.4 dB/100 km), IC-XT can significantly limit the transmission distance in MCF transmission. Although it may be possible to employ MCFs with lower XT [29], [30], they also highlight the need for a better understanding of dynamic crosstalk impairment for long distance transmission. Overall, these results show that efforts to reduce it or minimize its impact maybe crucial to fully exploit the potential resource sharing and integration benefits of MCF based SDM systems, while maintaining performance comparable with current single core fiber transmission.

2. Time Averaged Crosstalk Characterization 7-Core MCF

This section describes the single-span crosstalk characterization of the MCF used for re-circulating transmission, first performed in [26]. The set-up for measuring the core-to-core crosstalk for each core pair combination is shown in Fig. 1(a). Amplified spontaneous emission (ASE) noise with 5 nm bandwidth, centered at 1550.6 nm, was generated by concatenated erbium doped fiber amplifiers (EDFAs) and optical band pass filters (OBPFs). The ASE was switched individually to each core in turn. The output signal in the selected core and all other cores was then selected in turn using a second optical switch and measured with a high sensitivity optical power meter to produce the 7×7 coupling matrix of the core-to-core interactions of the fiber. The 28.35 km 7-core MCF had a step-index profile with a core-cladding index difference of 0.42%. It was spooled with an average diameter of 200 mm on a reel and had a core diameter, pitch, and cladding of 8.2 μm, 44.3 μm, and 160 μm, respectively. The mode field diameter at a wavelength of 1.55 μm amounted to 9.6 μm.

The core layout is shown in Fig. 1(b). Fig. 1(c) shows the summed crosstalk contribution of all other cores to each core as well as the measured insertion loss for each core including connector loss. As expected, the aggregated crosstalk depends on the number of neighboring cores and is highest for the center core and roughly equal for each of the outer cores sharing fewer neighboring cores at the minimum core pitch. This is confirmed from Fig. 1(d), which shows the individual crosstalk contribution between each core pair. The range of crosstalk contributions to the centre core from each outer core is fairly uniform varying by less than 2 dB. The crosstalk in the outer cores is dominated by the center and neighboring outer cores, which is between 8 dB and 14 dB higher than the contribution from non-adjacent outer cores. The centre core shows the worst XT performance with a combined XT power of –34.9 dB/span, compared to –37.6 dB/span to –39 dB/span for the outer cores, giving an average XT power

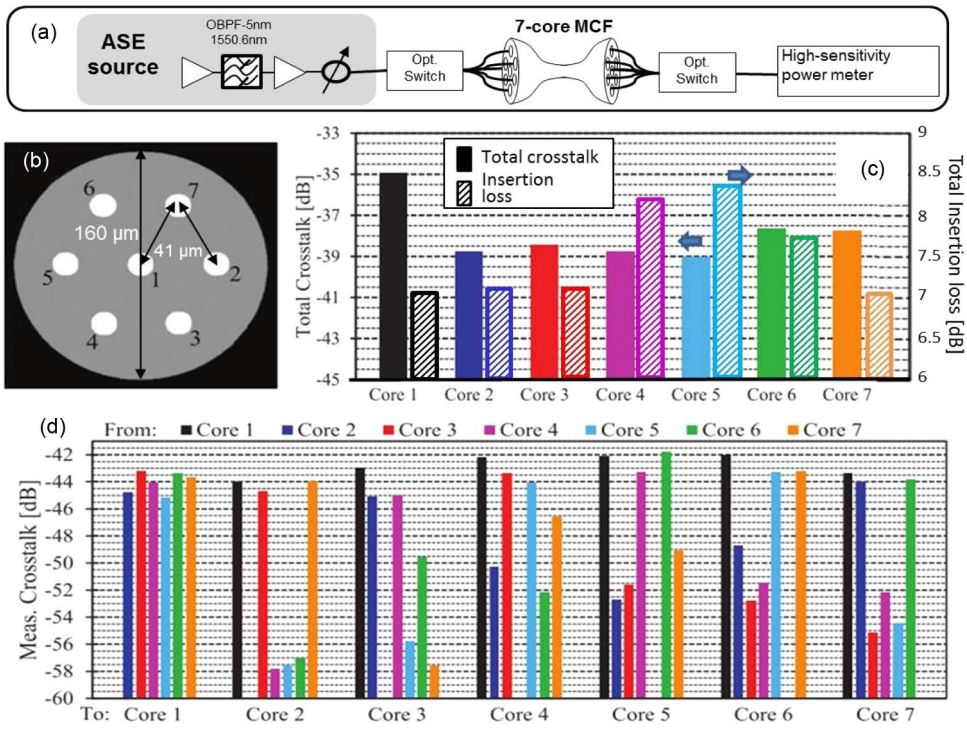

Fig. 1. (a) Experimental set-up for crosstalk measurements, (b) core configuration of the 28.35 km 7-core fiber, (c) total-crosstalk power and insertion loss per core including connector contributions, and (d) measured pairwise crosstalk power between cores.

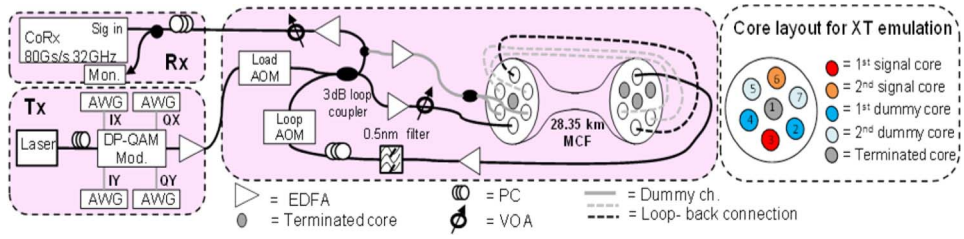

Fig. 2. Experimental set-up for transmission measurements as a function of inter-core XT from dummy channels.

of all seven cores of –37.7 dB/span or –32.2 dB/100 km. The connectors were already spliced to the fiber on delivery and it was not possible to independently measure their XT contribution, although we note that couplers based on the same design principles showed core-to-core XT between –50 dB and –65 dB, a coupling loss of 0.3 dB, and lower than –50 dB back reflection.

3. Experimental Set-Up for BER Measurements of Inter-Core Crosstalk Limited Transmission

Various MCFs with different core layout, core pitch, and cladding refractive index profiles and various strategies for reducing the crosstalk interaction and its impact have been proposed [2], [4]–[8], [19]–[21]. Hence, to emulate a wide range of potential crosstalk values, the set-up shown in Fig. 2, based on a recirculating transmission loop, was used. The signal laser was a 100 kHz linewidth external cavity laser tuned to 1550.116 nm and modulated in a dual parallel Mach-Zehnder modulator, referred to as DP-QAM modulator in Fig. 2. The modulator was

driven by four independent arbitrary waveform generators (AWGs). Each AWG had an analogue bandwidth of 14 GHz and used a sampling rate of 50 GS/s to generate pre-equalized PDM-QPSK, PDM-16QAM and PDM-64QAM signals at 25 GBd with a root-raised cosine pulse shape and a roll-off of 0.01. After modulation, an EDFA boosted the signal power before transmission over the 7-core MCF. Each loop recirculation used two opposite outer cores (cores 3 and 6) of a 28.35 km MCF span giving a total length of 56.7 km and round trip time of 278 μs.

The core arrangement for transmission is also shown as an inset in Fig. 2. The loop contained two further EDFAs and 100 GHz bandwidth optical filter to limit ASE with optical taps and variable optical attenuators (VOAs) used for setting and monitoring the launch power into each core. IC-XT was emulated by using dummy channels generated from the loop output after each recirculation. The dummy channels were amplified and decorrelated with fiber patch cords before being re-injected into the appropriate fiber cores. Since the IC-XT in any core is dominated by the adjacent cores, dummy channels were injected into cores 2 and 4, neighboring the first signal core 3, with the output of these cores then fed-back to cores 7 and 5, adjacent to the second signal core 6. Since the center core is adjacent to all other cores, no signal was injected to simplify XT calculations. Tapping the dummy channels from the loop output ensured that they had transmission and noise degradation similar to the signal channels, closely emulating a real MCF link.

Without any power in the dummy channels, the XT originating from only the other signal core was estimated to be 47.9 dB per 56.7 km recirculation or –45.4 dB/100 km. The signal power was maintained at the optimum launch power of 0 dBm for each format during all measurements and the launch power of the dummy channels varied from –9 dBm to +9 dBm to give a range of XT/span values of –45.9 dB to –27.9 dB, equivalent to –43.4 dB to –25.4 dB per 100 km.

Acousto-optic modulators (AOMs) were used to control the input and recirculation time in the loop with a common timing control used to gate the AOMs and trigger the receiver for reception after the required recirculation time. At the loop output, the receiver path contained an EDFA, a polarization controller (PC) and a VOA for polarization and power control. For all measurements, signal detection was performed in a polarization-diverse optical coherent receiver (CoRx) connected to a digital sampling oscilloscope with 32 GHz analog bandwidth operating at 80 GS/s. Offline processing was used to recover the signal, consisting of resampling to 50 GS/s, followed by normalization and dispersion compensation. Polarization de-multiplexing was performed using a multiple-input-multiple output (MIMO) structure whose equalizers were 17-tap filters updated using a decision-directed least-mean squares (DD-LMS) algorithm with carrier frequency offset and phase recovery performed in the equalizer loop. All bit-error rate (BER) measurements were calculated from the average of three traces, each containing at least 250000 symbols.

4. Measurements of Crosstalk Limited Transmission

Fig. 3(a)–(c) shows the measured BER as a function of transmission distance with different levels of XT, normalized to a 100 km fiber span, for PDM-QPSK, PDM-16QAM, and PDM-64QAM, respectively. Fig. 3(d) summarizes the results by comparing the maximum transmission distances of each format at three different BER thresholds of 1×10^{-3}, 3.8×10^{-3}, commonly used as the threshold for hard-decision forward error correction (FEC), and 1.5×10^{-2}, often used as the BER threshold for soft-decision FEC.

Evident from Fig. 3 is that increasing the level of IC-XT per span has an increasingly detrimental impact on the transmission distance for all QAM formats. For the highest XT level of –25.4 dB/100 km and at BER $= 1.5 \times 10^{-2}$ the maximum transmission distance for PDM-QPSK of around 7000 km is reduced to 2800 km and for the same BER the PDM-16QAM distance is reduced from around 2400 km to 800 km. For PDM-64QAM transmission, at the same XT level prevents reaching even two recirculations (113.4 km) for a BER below 1.5×10^{-2}, showing that the impact of XT is even more severe for higher order QAM formats which are more sensitive to noise.

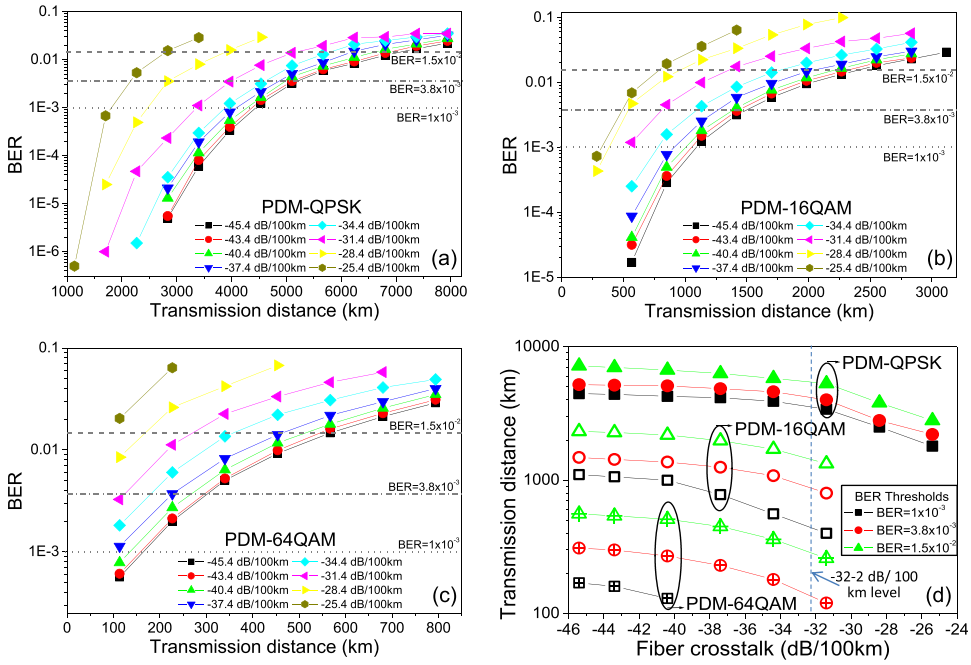

Fig. 3. BER vs transmission distance for different XT levels (per 100 km transmission) for 25 GBd (a) PDM-QPSK, (b) PDM-16QAM, (c) PDM 64QAM, and (d) transmission distance vs IC-XT level for BER thresholds of $1 \times 10 - 3$, $3.8 \times 10 - 3$, and $1.5 \times 10 - 2$.

This is also observed by comparing the transmission distances corresponding to the average crosstalk per span of –32.2 dB/100 km, which corresponds to the average XT level that can be expected for signals with equal launch power in each core in this fiber. At this XT level, for a BER $= 1.5 \times 10^{-2}$ the transmission distance decreases compared to the signal only case are 24%, 38%, and 54% for QPSK, 16QAM, and 64QAM, respectively. For a BER $= 3.8 \times 10^{-3}$, these figures become 18%, 40%, and 56% for QPSK, 16QAM, and 64QAM, respectively, again showing an increasing impact on transmission distance for the higher modulation order formats.

These results show that reducing and managing IC-XT becomes crucial if these fibers are to be used for long-haul transmission. In addition to system techniques such as bi-directional transmission [19] fiber design features such as using a refractive index trench around each core to improve the confinement of the optical field maybe required to avoid unmanageable cladding diameters to accommodate a larger core pitch. MCFs with a heterogeneous core design are good candidates for long-haul transmission with IC-XT below the measured range potentially able to minimize IC-XT impairment. Furthermore, the XT in such fibers does not increase with bending radius and may allow higher core-count fibers without requiring a larger core-pitch [29]. However, the MCF with lowest reported IC-XT to date [30] (≈64.7 dB/100 km at 1550 nm) used a homogeneous core-design and the matching propagation delay between cores in such fibers may make them attractive in MCF systems [15], [16], [31].

5. Impact of Dynamic Crosstalk Characteristics

The previous section investigated the impact of non-varying average distributed crosstalk in MCF transmission. However, unlike localized crosstalk, the distributed crosstalk in MCFs has been shown to possess a random behavior [23], [24] which should be analyzed over many hours or days to fully quantify its impact. The aim of this section is not to make quantitative predictions of the impact of such crosstalk but to demonstrate the potential for the dynamic nature of crosstalk to place a further performance limitation on the long term operation of MCF fiber and highlight the need for much more detailed analysis. Using an existing model [23], [24] and

assuming a system limited by IC-XT from a single core, we give an expression for the outage probability and use this to calculate an additional OSNR requirement to guarantee an outage probability of 1×10^{-5} in the presence of dynamic crosstalk fluctuations.

We begin by considering the time or wavelength evolution of crosstalk in a MCF, as characterized by a cumulative distribution function (CDF) derived in [23], where X_μ is the average crosstalk, to be

$$F(X) = 1 - \left(1 + \frac{2X}{X_\mu}\right)\exp\left(\frac{4X}{X_\mu}\right). \tag{1}$$

The impact of time varying crosstalk on the performance of QAM signals has been previously addressed in [23], assuming that the stochastic behavior of crosstalk translates into a randomly varying Q-factor. Here, we propose a simpler approach, assuming that the crosstalk is small enough to characterize as an additional noise affecting the OSNR of the signal under analysis and varying much slower than the signal symbol rate. We can then approximate the required OSNR of a crosstalk-degraded signal as

$$\mathrm{OSNR}_{XT} = \frac{P_s}{(2S_{\mathrm{ASE}} + S_{XT})\delta f} = \left(\mathrm{OSNR}^{-1} + S_{XT}\frac{\delta f}{P_s}\right)^{-1} \tag{2}$$

where OSNR is the OSNR in the absence of crosstalk, P_s is the signal power, S_{ASE} is the single-polarization power spectral density of the ASE noise, and δf is the resolution bandwidth. The term S_{XT} is the power spectral density of the crosstalk, which is assumed flat within the signal bandwidth and approximated by

$$S_{XT} = X\frac{P_s}{R_s} \tag{3}$$

with R_s as the symbol rate and X as the random varying crosstalk. Replacing (3) in (2) yields

$$\mathrm{OSNR}_{XT} = \left(\mathrm{OSNR}^{-1} + X\frac{\delta f}{R_s}\right)^{-1}. \tag{4}$$

As such, in order to have the crosstalk-degraded signal reaching the required OSNR in the presence of this dynamic crosstalk term, the OSNR can be increased by the OSNR penalty given by

$$\Delta\mathrm{OSNR} = \left(1 - \mathrm{OSNR}_{\mathrm{req}}X\frac{\delta f}{R_s}\right)^{-1} \tag{5}$$

where the $\mathrm{OSNR}_{\mathrm{req}}$ is the required OSNR in the absence of crosstalk to reach a given BER threshold. Fig. 4 shows the OSNR penalty for the considered modulation formats and BER thresholds as a function of the crosstalk level for the same BER thresholds used in the transmission measurements of 1×10^{-3}, 3.8×10^{-3}, and 1.5×10^{-2}. By inverting (5), we can determine threshold values for the crosstalk assuming a maximum allowed OSNR penalty of 1 dB. Table 1 summarizes the $\mathrm{OSNR}_{\mathrm{req}}$ values and crosstalk thresholds obtained for QPSK, 16QAM and 64QAM at 25 Gbd. The higher crosstalk threshold for a 1 dB penalty can then be used to calculate the achievable transmission distance for each format as also shown in Table 1, assuming a crosstalk of –32.2 dB/100 km, the average crosstalk level of the 7-core fiber used for transmission measurements with equal launch power in each core. In comparison with the experimental results presented in the Section 4, the limitation on transmission distance is underestimated. This can be explained by inspection of the plots in Fig. 3(a)–(c), where it is clear that crosstalk is not the dominant impairment for values above –37.4 dB since changing the crosstalk level has little impact on the reach. In these cases, the dominant limitation can be considered non-linear impairment and noise interactions, and hence, it is not possible to reach the maximum transmission distance of a system limited only in inter-core crosstalk.

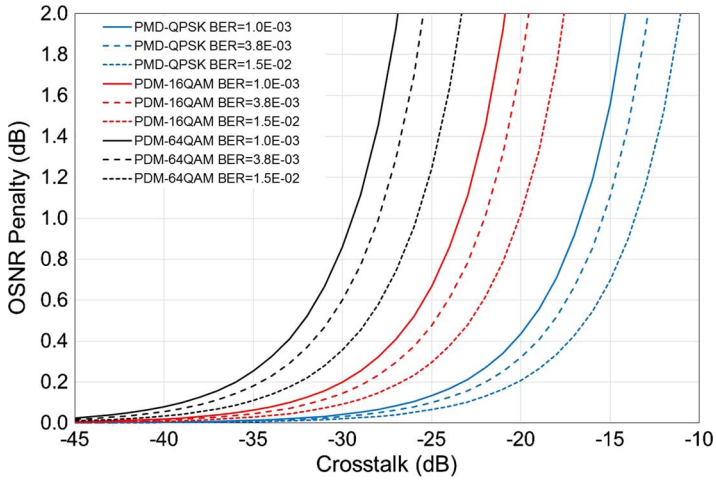

Fig. 4. OSNR penalty due to crosstalk for PDM-QPSK, PDM-16QAM, and PDM 64QAM at 25 Gbd for BER thresholds of 1×10^{-3}, 3.8×10^{-3}, and 1.5×10^{-2}.

TABLE 1

Required OSNR, Maximum Crosstalk Levels for and Maximum Average Crosstalk for Outage Probability of 1×10^{-5}

Format	Required OSNR	Crosstalk for 1dB penalty	Reach for 1 dB crosstalk penalty*	Maximum tolerable crosstalk for 1×10^{-5} outage probability	Reach with $<1\times10^{-5}$* outage probability
QPSK, BER=1×10^{-3}	9.7 dB	-16.6 dB	3631 km	-21.9 dB	1072 km
QPSK, BER=3.8×10^{-3}	11.5 dB	-15.6 dB	4571 km	-20.9 dB	1349 km
QPSK, BER=1.5×10^{-2}	12.8 dB	-13.8 dB	6918 km	-19.1 dB	2042 km
16-QAM, BER=1×10^{-3}	16.2 dB	-23.6 dB	724 km	-28.9 dB	214 km
16-QAM, BER=3.8×10^{-3}	18.2 dB	-22.2 dB	1000 km	-27.5 dB	295 km
16-QAM, BER=1.5×10^{-2}	19.5 dB	-20.2 dB	1585 km	-25.5 dB	468 km
64-QAM, BER=1×10^{-3}	22.0 dB	-29.6 dB	182 km	-34.9 dB	54 km
64-QAM, BER=3.8×10^{-3}	24.1 dB	-28.1 dB	257 km	-33.4 dB	76 km
64-QAM, BER=1.5×10^{-2}	25.6 dB	-26.0 dB	417 km	-31.3 dB	123 km

* Assuming an average crosstalk of -32.2 dB/100km

A more realistic approach may be taken by assuming that there is a finite probability that the crosstalk will exceed the maximum allowed level for a given average crosstalk level. This probability is given by taking the survival function 1-F(X) from (1). Therefore, we can estimate the maximum level of average crosstalk that is tolerable for a given outage probability. By inverting the crosstalk CDF presented in (1) and using a Taylor series expansion, it may be shown that the maximum allowed average crosstalk in logarithmic units can be approximated by

$$[X_\mu]_{\text{dB}} \approx [X_{\text{max}}]_{\text{dB}} - 10\log_{10}\left[0.4431 - \frac{\ln(P_o)}{4}\right] \tag{6}$$

where X_{max} is the highest tolerable time-averaged crosstalk, and P_o is the outage probability. The result expressed in (6) shows that the practical impact of the random behavior of crosstalk in MCFs can be translated into a maximum average crosstalk requirement 5.3 dB lower than that which would be expected for a localized crosstalk source, assuming an acceptable outage probability of 1×10^{-5} [28]. The values of maximum tolerable time averaged crosstalk for the considered modulation formats and BER thresholds are also shown in Table 1 along with a revision of the maximum reach values calculated for these conditions. Table 1 shows that for this

particular case, the additional OSNR required to guarantee an outage probability of 1×10^{-5} in the presence of dynamically varying crosstalk significantly reduces the achievable transmission distance below that achieved experimentally in Section 4. We stress here, that the model used can be considered only as a conservative estimation, assuming crosstalk being the only impairment and from only a single core, as opposed to aggregated crosstalk from two neighboring cores as used in the experimental measurements of Section 4 here and at least three neighboring cores in a fully loaded 7 core MCF. We also note that these dynamic crosstalk effects have yet to be observed over more than one MCF span and how the observed statistics of crosstalk variation hold after long distance fiber transmission leading to the predicted behavior has yet to be experimentally verified. Furthermore, the combined interference from multiple cores may require a new evaluation of the statistical properties of the combined crosstalk and is not the aim of this analysis.

These results show that, although the average crosstalk values required for long distance transmission of QAM formats reported in the previous section are valid over short periods of time, they may not guarantee a quality of service over longer periods. The role of dynamic crosstalk effects may require additional overhead compared to the average XT measurements and lead to substantially higher OSNR requirements in order to maintain an acceptable outage probability. We note that although we are not aware of any such evaluation of these effects for QAM signals, the impact of such dynamic effects in a single span of MCF have been experimentally investigated for OFDM signals [32], where the random crosstalk-induced performance fluctuations lead to a significant decrease of the overall system performance. If such phenomena is shown to be a feature of long-distance MCF transmission, it may be that transmission schemes able to adapt to fluctuating crosstalk conditions, such as high-dimensional coded modulation formats [16], [33], [34], may become important to exploit MCF systems, but primarily this analysis serves to highlight the need for a better understanding of the impact of IC-XT in long distance MCF links.

6. Conclusion

We have investigated the impact of inter-core crosstalk on the transmission distance of square QAM modulation formats in multi-core fibers. We have experimentally measured the impact of varying crosstalk levels on the achievable transmission distance of 25 GBd PDM-QPSK, PDM-16QAM and PDM-64QAM modulation formats in a 7 core fiber. We observed that, although it may not be problematic for short reach and data-centre networks, inter-core crosstalk exceeding 40 dB/100 km can significantly limit the transmission distance for all three formats. For the homogeneous 7-core fiber used in these measurements, a crosstalk level equivalent to equal launch power in all cores (–32.2 dB/100 km) limits the transmission distance by 24%, 38% and 54% for BER $= 1.5 \times 10^{-2}$ and 18%, 40%, and 56% at BER $= 3.8 \times 10^{-3}$ for PDM-QPSK, PDM-16QAM, and PDM-64QAM, respectively, showing that the impact of crosstalk on transmission distance is more severe for higher order formats. Finally, we investigated the potential for an additional impact of inter-core crosstalk on the long term service of MCF links by considering additional reach limitation caused by higher required receiver signal to noise ratio to guarantee a specific outage probability in the presence of crosstalk spikes arising from dynamic properties of inter-core crosstalk. Overall these results show that adequate management of inter-core crosstalk is crucial for long-haul multi-core fiber transmission and that fiber designs with low intrinsic crosstalk, such as those with heterogeneous core design, may be more suitable for long distance transmission. Although, more detailed studies are required to fully quantify its impact, these results show that careful design of such systems should consider both the average level and dynamic properties of crosstalk to achieve optimum performance.

Acknowledgment

The authors thank the NICT technical staff for assistance with experiments.

References

[1] D. J. Richardson, J. M. Fini, and L. E. Nelson, "Space-division multiplexing in optical fibres," *Nat. Photon.*, vol. 7, pp. 354–362, 2013.
[2] H. Takahashi, K. Igarashi, and T. Tsuritani, "Long-haul transmission using multicore fibers," in *Proc. Opt. Fiber Commun. Conf.*, San Francisco, CA, USA, Mar. 2014, pp. 1–3.
[3] Y. Lee, K. Tanaka, E. Nomoto, H. Arimoto, and T. Sugawara, "Multi-core fiber technology for optical-access and short-range links," in *Proc. Int. Conf. Opt. Internet*, Jeju, Korea, Aug. 2014, pp. 1–2.
[4] B. Zhu *et al.*, "112-Tb/s space-division multiplexed DWDM transmission with 14-b/s/Hz aggregate spectral efficiency over a 76.8-km seven-core fiber," *Opt. Exp.*, vol. 19, no. 17, pp. 16, pp. 16665–16671, 2011.
[5] J. Sakaguchi *et al.*, "19-core fiber transmission of $19 \times 100 \times 172 - \mathrm{Gb/s}$ SDM-WDM-PDM-QPSK signals at 305 Tb/s," in *Proc. IEEE OFC/NFOEC*, 2012, pp. 1–3.
[6] K. Igarashi *et al.*, "Super-Nyquist-WDM transmission over 7,326-km seven-core fiber with capacity-distance product of 1.03 Exabit/s/km," *Opt. Exp.*, vol. 22, no. 2, pp. 1220–1228, Jan. 2014.
[7] H. Takara *et al.*, "1.01-Pb/s (12 SDM/222 WDM/456 Gb/s) crosstalk-managed transmission with 91.4-b/s/Hz aggregate spectral efficiency," presented at the Eur. Conf. Exh. Opt. Commun., 2012, paper Th.3.C.1.
[8] B. J. Puttnam *et al.*, "2.15 Pb/s transmission using a 22 core homogeneous single-mode multi-core fiber and wideband optical comb," in *Proc. IEEE ECOC*, 2015, pp. 1–3.
[9] Y. Tottori *et al.*, "Low loss optical connection module for seven-core multicore fiber and seven single-mode fibers," *IEEE Photon. Technol. Lett.*, vol. 24, no. 21, pp. 1926–1928, Nov. 2012.
[10] H. Takahashi *et al.*, "Impact of crosstalk in an arrayed-waveguide multiplexer on NxN optical interconnection," *IEEE J. Lightw. Technol.*, vol. 14, no. 6, pp. 1097–1105, Jun. 1996.
[11] W. Klaus, J. Sakaguchi, B. J. Puttnam, Y. Awaji, and N. Wada, "Free-space coupling conditions for multi-core few-mode fibers," in *Proc. IEEE Photon. Soc. Summer Topical Meet. Ser.*, 2014, pp. 182–183.
[12] K. S. Abedin *et al.*, "Multicore erbium doped fiber amplifiers for space division multiplexing systems," *J. Lightw. Technol.*, vol. 32, no. 16, pp. 2800–2808, Aug. 2014.
[13] Y. Tsuchida and R. Sugizaki, "Multicore erbium doped fiber amplifier for space division multiplexing," in *Proc. Photon. Soc. Summer Topical Meet. Ser.*, 2013, pp. 103–104.
[14] H. Ono, K. Takenaga, K. Ichii, and M. Yamada, "Amplification technology for multi-core fiber transmission," in *Proc. Photon. Soc. Summer Topical Meet. Ser.*, 2014, pp. 146–147.
[15] B. J. Puttnam *et al.*, "High-capacity self-homodyne PDM-WDM-SDM transmission in a 19-core fiber," *Opt. Exp.*, vol. 22, no. 18, pp. 21185–21191, Sep. 2014.
[16] B. J. Puttnam *et al.*, "Modulation formats for multi-core fiber transmission," *Opt. Exp.*, vol. 22, no. 26, pp. 32457–32469, Dec. 2014.
[17] R. Ryf *et al.*, "Mode-multiplexed transmission over conventional graded-index multimode fibers," *Opt. Exp.*, vol. 23, no. 1, pp. 235–246, 2015.
[18] N. K. Fontaine, "Characterization of multi-mode fibers and devices for MIMO communications," in *Proc. SPIE, Next-Gener. Opt. Commun., Components, Sub-Syst., Syst. III*, 2013, vol. 9009, pp. 1–8.
[19] A. Sano *et al.*, "Crosstalk-managed high capacity long haul multicore fiber transmission with propagation-direction interleaving," *J. Lightw. Technol.*, vol. 32, no. 16, pp. 2771–2779, Aug. 2014.
[20] K. Takenaga *et al.*, "Reduction of crosstalk by trench-assisted multi-core fiber," in *Proc. IEEE OFC/NFOEC*, 2011, pp. 1–3.
[21] T. Hayashi, T. Taru, O. Shimakawa, T. Sasaki, and E. Sasaoka, "Design and fabrication of ultra-low crosstalk and low-loss MCF," *Opt. Exp.*, vol. 19, no. 17, pp. 16576–16592, Aug. 2011.
[22] J. M. Fini, B. Zhu, T. Taunay, M. Yan, and K. Abedin, "Crosstalk in multi-core optical fibres," in *Proc. IEEE ECOC*, 2011, pp. 1–3.
[23] T. Hayashi, T. Sasaki, and E. Sasaoka, "Behavior of inter-core crosstalk as a noise and its effect on Q-factor in multi-core fiber," *IEICE Trans. Commun.*, vol. 97, no. 5, pp. 936–944, 2014.
[24] R. S. Luís *et al.*, "Time and modulation frequency dependence of crosstalk in homogeneous multi-core fibers," *IEEE J. Lightw. Technol.*, vol. 34, no. 2, pp. 441–447, Jan. 2016.
[25] P. Winzer, A. H. Gnauck, A. Konczykowska, F. Jorge, and J.-Y. Dupuy, "Penalties from in-band crosstalk for advanced optical modulation formats," in *Proc. IEEE ECOC*, Sep. 2011, pp. 1–3.
[26] T. A. Eriksson *et al.*, "Experimental investigation of crosstalk penalties in multicore fiber transmission systems," *IEEE Photon. J.*, vol. 7, no. 1, Feb. 2015, Art. ID 7200507.
[27] B. J. Puttnam *et al.*, "Impact of inter-core crosstalk on the transmission distance of QAM formats in multi-core fibers," in *Proc. Photon. Switch.*, Sep. 2015, pp. 55–57.
[28] P. J. Winzer and G. J. Foschini, "MIMO capacities and outage probabilities in spatially multiplexed optical transport systems," *Opt. Exp.*, vol. 19, no. 17, pp. 16680–16696, 2011.
[29] M. Koshiba, K. Saitoh, and Y. Kokubun, "Heterogeneous multi-core fibers: Proposal and design principle," *IEICE Electron. Exp.*, vol. 6, no. 2, pp. 98–103, 2009.
[30] T. Hayashi, T. Taru, O. Shimakawa, T. Sasaki, and E. Sasaoka, "Design and fabrication of ultra-low crosstalk and low-loss multi-core fiber," *Opt. Exp.*, vol. 19, no. 17, pp. 16576–16592, 2011.
[31] R. S. Luís *et al.*, "Comparing inter-core skew fluctuations in multi-core and single-core fibers," in *Proc. IEEE CLEO*, 2015, pp. 1–2.
[32] J. P. Rosário *et al.*, "Experimental assessment of the time-varying impact of multi-core fiber crosstalk on a SSB-OFDM signal," in *Proc. Photon. Switch.*, Florence, Italy, Sep. 2015, pp. 166–168.
[33] T. A. Eriksson *et al.*, "Single parity check-coded 16QAM over spatial superchannels in multicore fiber transmission," *Opt. Exp.*, vol. 23, no. 11, pp. 14569–14582, Jun. 2015.
[34] B. J. Puttnam *et al.*, "Linear block-coding across >5 Tb/s PDM-64QAM spatial-super-channels in a 19-core fiber," in *Proc. IEEE ECOC*, 2015, pp. 1–3.